

# Self-supervised Group Meiosis Contrastive Learning for EEG-Based Emotion Recognition

Haoning Kan  
Faculty of Science  
Beijing University of Technology  
Beijing, China  
KanHaoning@emails.bjut.edu.cn

Jiale Yu  
Beijing-Dublin International College  
Beijing University of Technology  
Beijing, China  
jiale.yu@ucdconnect.ie

Jiajin Huang  
Faculty of Information Technology  
Beijing University of Technology  
Beijing, China  
jhuang@bjut.edu.cn

Zihe Liu  
Faculty of Science  
Beijing University of Technology  
Beijing, China  
Zihe\_Liu@emails.bjut.edu.cn

Haiyan Zhou\*  
Faculty of Information Technology  
Beijing University of Technology  
Beijing, China  
zhouhaiyan@bjut.edu.cn

**Abstract**—The progress of EEG-based emotion recognition has received widespread attention from the fields of human-machine interactions and cognitive science in recent years. However, how to recognize emotions with limited labels has become a new research and application bottleneck. To address the issue, this paper proposes a Self-supervised Group Meiosis Contrastive learning framework (SGMC) based on the stimuli consistent EEG signals in human being. In the SGMC, a novel genetics-inspired data augmentation method, named Meiosis, is developed. It takes advantage of the alignment of stimuli among the EEG samples in a group for generating augmented groups by pairing, cross exchanging, and separating. And the model adopts a group projector to extract group-level feature representations from group EEG samples triggered by the same emotion video stimuli. Then contrastive learning is employed to maximize the similarity of group-level representations of augmented groups with the same stimuli. The SGMC achieves the state-of-the-art emotion recognition results on the publicly available DEAP dataset with an accuracy of 94.72% and 95.68% in valence and arousal dimensions, and also reaches competitive performance on the public SEED dataset with an accuracy of 94.04%. It is worthy of noting that the SGMC shows significant performance even when using limited labels. Moreover, the results of feature visualization suggest that the model might have learned video-level emotion-related feature representations to improve emotion recognition. And the effects of group size are further evaluated in the hyper parametric analysis. Finally, a control experiment and ablation study are carried out to examine the rationality of architecture. The code is provided publicly online<sup>1</sup>.

**Index Terms**—EEG-based emotion recognition, group-level representation, contrastive-learning, self-supervised learning, data augmentation, meiosis

## I. INTRODUCTION

Emotion plays a crucial role in human cognition and involves many application fields. For example, in the field of human-machine interaction [1], emotion recognition enables

the machine to provide more humanized interaction. In consumer neuroscience, emotion analysis is a common tool to obtain the user experience for product design [2]. Recently, the method of emotion recognition based on Electroencephalography (EEG) signal has shown its advantages. Compared to conscious behavior signals such as facial expression and body language, the EEG has the advantage of being difficult to hide or disguise. Compared with other physiological signals such as the fMRI (functional magnetic resonance imaging), and ECG (Electrocardiogram), the EEG is more convenient for sampling and has a higher time resolution.

There is great progress in the field of EEG-based emotion recognition. With traditional machine learning techniques, the handcrafted features are calculated and selected carefully, which is quite critical during emotion recognition. While these approaches rely too much on the researcher's experiences on EEG signals and cognitive related knowledge. In recent years, the development of deep learning methods achieves competitive accuracy, which could not pay attention to the handcrafted features. With the guidance of a large number of data with labels, the deep learning models would learn high-level emotion-related feature representation for precise affective computing [3]–[7].

Generally, artificial labels are crucial for training deep learning models based on the common supervised methods. But there is some condition requiring higher accurate and real-time recognition, obtaining qualified labels is expensive. For example, in neuroscience, EEG is frequently used to explore the process of emotion, such as in the tasks of empathy and reading comprehension. Participants are usually required to answer questions, so that the researchers could get their emotion situations. However, the emotion labels obtained through this way are time-consuming and laborious. And it is easy to generate subjective bias, which might decrease the reliability of labels [8], [9]. Similarly, in the application of consumer neuroscience, the EEG signals are recorded to

\*Corresponding author

<sup>1</sup> <https://github.com/kanhaoning/Self-supervised-group-meiosis-contrastive-learning-for-EEG-based-emotion-recognition>

evaluate the participants' emotional states while they are playing games, listening to music, and watching movies, and advertisements, which aims to provide instructive references to the content creator, [10]–[13]. In these conditions, the precise and time-intensive labels are also required. Therefore, the lack of qualified labels hinders the application of machine learning-based models in many precise fields.

Previous studies have explored to reduce the dependence on artificial labels [14], [15]. Several neuroscience studies have shown the exploitable consistency of stimuli in emotion EEG signals. They have discovered that the EEG signals among a group of subjects who watched the same emotional video clips share similar group-level stimuli-related features [16], [17]. Such features correlated with preference, arousal, valence, etc, are potential to make up for the lack of artificial labels. Existing methods mainly adopt the self-supervised learning (SSL) method to exploit such stimuli consistency. SSL can generate labels according to the attributes of data for learning. For example, Shen et al. proposed a novel contrastive learning framework [18] to learn representation by making the model maximizing the similarity between representations of EEG signals corresponding to the same stimuli. However, there exist random effects in the emotion-related EEG signals. For example, whether the subjects were distracted during the emotional tasks and their fatigue situations would increase the noise of the signals. And also the responses of participants could not be totally the same, which increases the difficulty in maximizing the similarity across subjects in contrastive learning.

To further improve the EEG-based emotion recognition under the SSL framework, we proposed a Self-supervised Group Meiosis Contrastive learning (SGMC) framework for EEG-based emotion recognition.

First, since larger samples could be better to represent the characteristics of signals from the view of statistics, we design a group projector in SGMC to collect a group of EEG samples to extract group-level representation for contrastive learning.

Second, we proposed a novel method of data augmentation to provides augmented group samples for contrastive learning. Applying data augmentation to enhance contrastive learning is a basic paradigm, however, there are few studies on augmenting group samples. Inspired by the meiosis mechanism in genetics [19], we augment data without changing stimuli features by pairing, cross exchanging, and separating. In this way, data augmentation enables contrastive learning further take the advantage of the alignment of stimuli in the EEG signal group. And then the SGMC enables the model learn critical representations and achieve competitive emotion recognition performance with a significant improvement. Here we summarize the contributions of this paper as follows:

- To reduce the dependence on emotion labels, we introduce a self-supervised contrastive learning framework to further exploit the consistency of stimuli for EEG-based emotion recognition.
- To decrease the effects of individual difference and random effects in EEG signals, we design a group-

based contrastive learning framework to extract group-level stimuli-related feature representations.

- To augment the group sample, we design a genetics-inspired data augmentation method, named Meiosis. It utilizes the alignment of stimuli to augment group samples without changing stimuli features. which provides augmented group samples to enhance contrastive learning.
- The SGMC achieves the state-of-the-art emotion classification results on the publicly available DEAP dataset with an accuracy of 94.72% and 95.68% in valence and arousal dimensions. On public SEED dataset also reaches competitive 94.04% accuracy, and achieve 91.01% accuracy fine-tuned with 50 labeled samples per category (0.14% of the full training set), exceeding 89.83% accuracy of fully-supervised learning with the full training set.

## II. RELATED WORK

### A. EEG-based Emotion Recognition

In earlier studies, emotional features of EEG signals were usually extracted to recognize by some traditional machine learning strategies. Such as the support vector machine (SVM) [20], Gaussian Naive Bayes classification [21], and k-nearest neighbor (k-NN) [22] are widely used classify emotion of the EEG signal.

Compared with the traditional machine learning method, the deep learning model has more advantages in extracting high-level emotional features. In recent years, more and more deep learning neural networks based on emotion recognition models achieved good performance on EEG-based emotion recognition tasks [3]–[7].

Recently popular methods focus on recurrent neural networks (RNNs/LSTMs), and convolutional neural networks (CNNs). In 2017, Alhagry et al [23] adopted a two-layer long-short term memory (LSTM) to reach satisfactory emotion classification with the input of the raw EEG signals. In 2020, Li et al [24] constructed model BiHDM adopted four RNN modules to capture the input of each hemispheric EEG electrode's data from horizontal and vertical streams and achieved the SOTA. CNN is also widely used for extracting spatial features of the EEG signal. In 2016, Li et al [25] proposed a hybrid network structure based on CNN and RNN for emotion recognition based on multi-channel EEG signals, which shown the effectiveness of a hybrid network in the trial-level emotion recognition tasks. In 2017, Alhagry et al. [26] explored a convolutional neural network and a simple deep neural network. This CNN model shown more significant performance and achieved the SOTA. In 2018 Shawky et al. [27] proposed a 3D CNNs model, which divides raw signals into 6-s segments to input. In the same year, Yang et al. [28] proposed a hybrid model combining CNN and RNN networks to learn spatial-temporal representation for emotion recognition. It utilized a sparse matrix as input to reflect the relative position of the electrodes. Compared with complex input of RNNs and 2D/3D CNNs, Cheah et al. [29] proposed a 1D-CNN based ResNet18, which adopted simple

input(channel  $\times$  time) to train the deeper neural network. It is more suitable to perform pre-training with simple data processing and a faster training process.

### B. Self-supervised Learning

Self-supervised learning aims to learn representation without relying on artificial labels. The latest research in the field of machine learning and deep learning shown the potential of the SSL method in learning generalized and robust representations [30]–[35]. SSL has been widely used in many fields. For example, in computer vision (CV), Gidaris et al. [30] based on spatial properties designed an SSL task to rotate the original image and require the model to predict the rotation angle. Based on the temporal properties of the video, an SSL task [31] was designed to require the model to predict whether the two video frames are close in time. In natural language processing (NLP), *word2vec* [32] designed SSL tasks such as predicting headword and adjacency words, etc. *BERT* [33] designed two SSL tasks masked language prediction and next sentence prediction, and achieved SOTA on 11 NLP tasks. In EEG signal processing, Zhang et al. [36] applied Generative Adversarial Network to design the SSL method. It makes the generator augment masked original signals to get simulated signals and requires the model to distinguish real and simulated signals, which alleviates the problem of EEG data scarcity and achieves SOTA.

Recently contrastive-learning-based SSL has made progress in EEG signal processing. Contrastive learning defines any two samples with internal relations as the positive pair, otherwise, it is the negative pair, whose loss function aims to maximize the similarity of representations between positive pairs minimums the similarity of representation between negative pairs. Shen et al. [18] proposed a self-supervised contrastive learning framework CLISA to improve inter-subjects prediction, which requires the model to predict whether two EEG signals are recorded when two subjects watch the same video clip. In this way, the model learned well inter-subject representation ability and achieved SOTA in inter-subject prediction after fine-tuning. In [14] several self-supervised contrastive learning methods were proposed to improve performance on limited label sample tasks. Among them, Relative Positioning (RP) requires the model to predict whether the two EEG signals are recorded in close time, and Contrastive Predictive Coding (CPC) requires the model to predict the representation of adjacent EEG signals via the anchor signal. They confirmed that models learned physiologically and clinically meaningful feature representations by SSL pre-training without label guidance. Further, they fine-tuned the pre-trained model to significantly outperformed the fully-supervised baseline on less labeled sample learning tasks. In [15] an augment-based SSL method is proposed, which requires the model to predict whether two augmented EEG signals come from the same original signal. It applies classical data augmentation such as time warping permutation and crop&resize and so on. The generalization ability of the model has significantly improved and exceeded

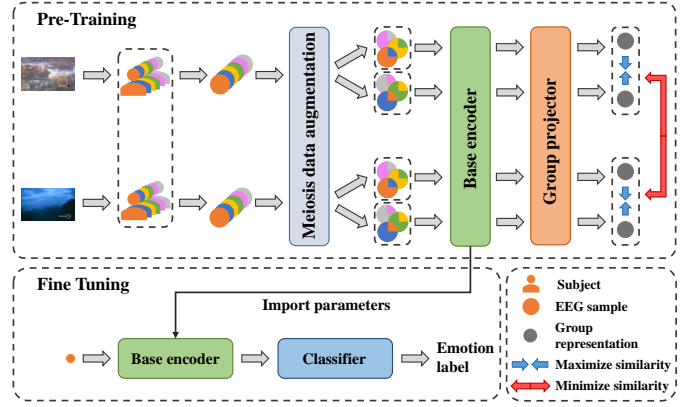


Fig. 1. Illustration of the proposed SGMC. During the process of pre-training, each group of samples is sampled from EEG samples corresponding to the same video clip stimuli. Then each group of EEG samples is augmented by genetics inspired Meiosis data augmentation to generate two augmented group samples. Each augmented group is sent to the base encoder to extract individual representations of each individual sample and then the group projector aggregates them to obtain the group-level representation. The model is required to maximize the similarity of representations between groups sharing the same stimuli and minimize the representations of groups that correspond to the different stimuli for minimizing the contrastive loss. The pre-trained base encoder will be fine-tuned with a classifier for emotion recognition.

fully-supervised learning in both the full and the limited labeled sample learning on sleep staging. Contrastive learning shows its excellence in improving inter-subject prediction, learning physiological feature representation without labels, and so on in EEG signal processing.

## III. PROPOSED METHOD

### A. Overall Framework

This paper designs a Self-supervised Group Meiosis Contrastive learning (SGMC) framework for EEG-based emotion recognition. As illustrated in Fig.1 the proposed framework consists of a contrastive learning pre-training process and an emotion recognition fine-tuning process. In the pre-training process, SGMC contains five components: a group sampler, the Meiosis data augmentation, a base encoder, a group projector, and a contrastive loss function. Firstly, the group sampler generates a minibatch containing several groups of EEG signals for augmenting. Secondly, the Meiosis augments each EEG group to generate two groups for constructing the positive and negative pairs. Nextly the base encoder extracts individual-level stimuli-related representations from each EEG signal. Then the group projector aggregates each group of representations to extract group-level stimuli-related representations and map them into another latent space for computing the similarity. Together, the parameters of the base encoder and group projector are optimized by minimizing the contrastive loss. In the fine-tuning process, the model that consisted of the pre-trained base encoder and initialized classifier performs the emotion classification training.

## B. Group Sampler

Generally, it is difficult to contrastive learning through extracting stimuli-related features from individual EEG samples. So we take the strategy of extracting from group EEG samples, to achieve it we construct the sampler to provide input for the minibatch.

In the processed dataset, video clips and subjects correspond to two axes of the dataset tensor. Among it, each EEG sample was defined as  $\mathbf{X}_v^s \in \mathbb{R}^{M \times C}$ , corresponding to a 1-second signal recorded when subject  $s$  watched a 1-second video clip  $v$ , where  $M$  is the number of times samples and  $C$  is the dimension of signals (*e.g.*, channels). To obtain a minibatch, illustrated in Fig.2 sampler first randomly sample  $P$  video clips  $v_1, v_2, \dots, v_P$  that have not been sampled in the current epoch. To sample two equal sample groups to construct positive pair for each clip stimuli, sampler nextly randomly select  $2Q$  subjects  $s_1, s_2, \dots, s_{2Q}$  to prepare for grouping. Further sampler extract the EEG signals corresponding to selected subjects and video clips,  $2PQ$  samples  $\mathcal{D} = \{\mathbf{X}_{v_i}^{s_k} | i = 1, 2, \dots, P; k = 1, 2, \dots, 2Q\}$  are obtained, which were recorded by  $2Q$  subjects when watched  $P$  video clips respectively. Furthermore, we note a group samples  $\mathbf{G}_i = \{\mathbf{X}_{v_i}^{s_1}, \mathbf{X}_{v_i}^{s_2}, \dots, \mathbf{X}_{v_i}^{s_{2Q}}\}$  corresponding to the video clip  $v_i$ . Among  $\mathbf{G}_i$ , each individual sample shared the similar -related features. In this way, sampler would provide the minibatch with  $P$  group samples  $\{\mathbf{G}_1, \mathbf{G}_2, \dots, \mathbf{G}_P\}$  corresponding to  $P$  different stimuli for pre-training.

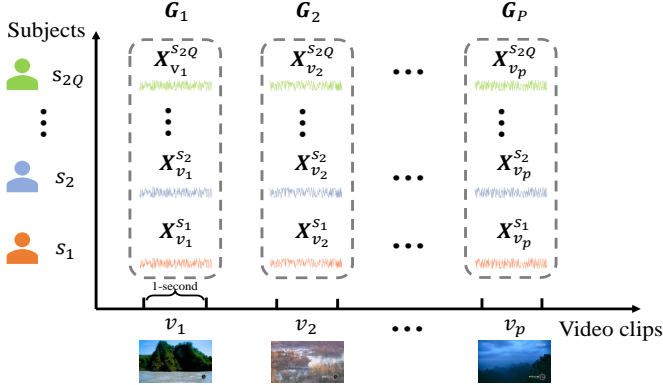


Fig. 2. The illustration of sampling for a minibatch. Sampler first samples  $P$  video clip and  $2Q$  subjects. For each sampled video clip, next the sampler samples a group of EEG signals recorded when sampled  $2Q$  subject watched it. Then  $P$  groups of EEG samples are obtained for a minibatch.

## C. Meiosis Data Augmentation

Meiosis aims to augment one group sample to generate two groups that preserve the same stimuli-related features by utilizing the alignment of stimuli in the EEG group for constructing the positive pair.

To increase the meaningful difficulty of the model decoding EEG samples, we hope to mix signals of different subjects. Moreover, to preserve the original stimuli-related features for extraction by SGMC, we select the signals corresponding to

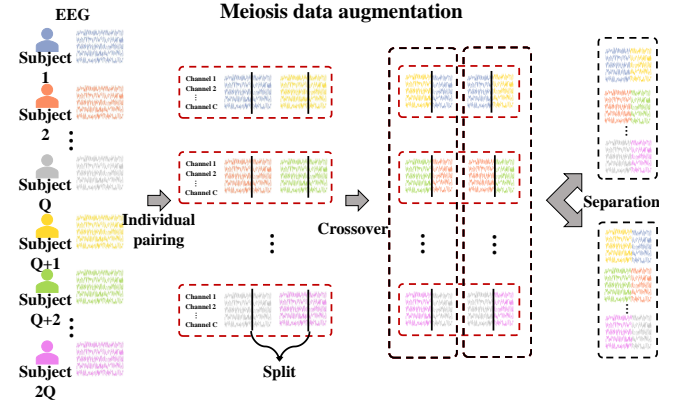


Fig. 3. The illustration of the Meiosis data augmentation. A group of EEG samples sharing the same stimuli are randomly paired and cross exchanged a part of the signal in a pair, and then separated into two groups.

the same stimuli to split and splice. So we design the crossover transformation as follows:

We represent  $\{a_1, a_2, \dots, a_M\}$  as any EEG signal  $\mathbf{A}$ , where  $a_i$  is the data at  $i^{th}$  sampling point ( $i=1,2,\dots,M$ ). Similarly represent  $\{b_1, b_2, \dots, b_M\}$  as any other signal  $\mathbf{B}$ . Further we exchange the data of the first  $c$  sampling points of two samples  $\mathbf{A}$  and  $\mathbf{B}$  to obtain  $\tilde{\mathbf{A}} = \{b_1, b_2, \dots, b_c, a_{c+1}, a_{c+2}, \dots, a_M\}$  and  $\tilde{\mathbf{B}} = \{a_1, a_2, \dots, a_c, b_{c+1}, b_{c+2}, \dots, b_M\}$ , where  $c$  is given. Such transformation for any two EEG signals is encapsulated as the following function expression:

$$\{\tilde{\mathbf{A}}, \tilde{\mathbf{B}}\} = T(\mathbf{A}, \mathbf{B}, c) \quad (1)$$

Furthermore, to take the advantage of the diversity of group combinations, we can randomly pair for crossover and separating. As illustrated in Fig.3 the overall Meiosis data augmentation can be designed as follows:

1) Individual pairing: For one original EEG signals group  $\mathbf{G}_i = \{\mathbf{X}_{v_i}^{s_k} | k = 1, 2, \dots, 2Q\}$  (corresponding to a video clip  $v_i$ ) individual signals are randomly paired to form  $Q$  pairs  $\{\mathbf{X}_{v_i}^{s_1}, \mathbf{X}_{v_i}^{s_{1+Q}}\}, \{\mathbf{X}_{v_i}^{s_2}, \mathbf{X}_{v_i}^{s_{2+Q}}\}, \dots, \{\mathbf{X}_{v_i}^{s_Q}, \mathbf{X}_{v_i}^{s_{Q+Q}}\}$  for crossover.

2) Crossover : Meiosis receives a randomly given split position  $c$  to perform transformation (1) for each pairs to obtain  $\{\{\tilde{\mathbf{X}}_{v_i}^{s_k}, \tilde{\mathbf{X}}_{v_i}^{s_{k+Q}}\} | k = 1, 2, \dots, Q\}$ .

3) Separation: The transformed signals are randomly divided into two groups, and paired transformed signals are required enter into the different groups  $\mathbf{A}$  and  $\mathbf{B}$ . Two homologous groups of EEG  $\tilde{\mathbf{G}}_i^A = \{\tilde{\mathbf{X}}_{v_i}^{s_k} | k = 1, 2, \dots, Q\}$  and  $\tilde{\mathbf{G}}_i^B = \{\tilde{\mathbf{X}}_{v_i}^{s_k} | k = Q + 1, Q + 2, \dots, 2Q\}$  can be obtained that sharing the similar group-level stimuli-related features.

Such data augmentation for group sample we represent it as follows function expression:

$$\{\tilde{\mathbf{G}}_i^A, \tilde{\mathbf{G}}_i^B\} = Meiosis(\tilde{\mathbf{G}}_i) \quad (2)$$

When Meiosis is built, for one minibatch of  $P$  group samples  $\mathcal{G}$ ,  $2P$  group samples  $\tilde{\mathcal{G}}$  can be obtained as follows:

$$\tilde{\mathcal{G}} = \{\tilde{\mathbf{G}}_i^t | i = 1, 2, \dots, P; t \in \{A, B\}\} = \text{Meiosis}(\mathcal{G}) \quad (3)$$

$\tilde{\mathbf{G}}_i^A$  could form a positive pair with  $\tilde{\mathbf{G}}_i^B$ , form negative pairs with any other  $2(P-1)$  group samples.

#### D. Base Encoder

To extract group-level stimuli-related features for contrastive learning, we first design a base encoder to extract individual-level stimuli-related features from each individual EEG sample. We introduce the base encoder  $f: \mathbb{R}^{M \times C} \rightarrow \mathbb{R}^D$  which map individual EEG sample  $\mathbf{X}$  to its representation  $\mathbf{h}$  on a 512-dimensional feature space. Based on the existing model ResNet18-1D [29], the base encoder is designed as follows:

As illustrated in Fig.4. It mainly contains 17 convolutional layers (Conv) with a 1D kernel. The kernels of the first convolutional layer parallel the time axis of the EEG signal tensor with a length of 9. Each residual block contains two convolutional layers with the same number and length of the kernels. In each residual block, kernels of the first layer parallel the time axis of the input EEG tensor, and the second layer parallels the channel axis. For the eight residual blocks, the length of the kernels is 15, 15, 11, 11, 7, 7, 3, and 3 in descending order. Max pooling with the 1D kernel (Maxpool), Avg pooling with the 1D kernel (Avgpool), Batch Normalization (BN), and Rectified Linear Unit (RELU) layers are shown in the corresponding positions in the figure.

Through the base encoder, for a augmented group sample  $\tilde{\mathbf{G}}_i^t$ , its individual-level stimuli-related representation set  $\{\mathbf{h}_1, \mathbf{h}_2, \dots, \mathbf{h}_Q\}$  can be obtained as by:

$$\mathbf{H}_i^t = f(\tilde{\mathbf{G}}_i^t) \quad (4)$$

The set is used for further extracting group-level features. The individual representations can also be used for extracting emotional features for emotion classification.

#### E. Group Projector

The group projector aims to accurately project stimuli-related representations into latent space from just 1-second EEG signals for calculating the similarity of video clip stimuli. To alleviate the hinders in extracting stimuli-related features from individual samples (fatigue, distraction, etc), the group projector is designed to extract group-level features from multiple samples.

A group of samples is an unordered set of matrixes that lacks a special extraction method. Most models focus on regular input representations. Such as the input of multi-channel images, there is a fixed order between different channels, as well as video, there is a fixed sequence between different frames. In the problem of unordered point cloud classification, [37] proposed PointNet adopting the symmetric function to build a network realized the features extraction of the unordered point cloud.

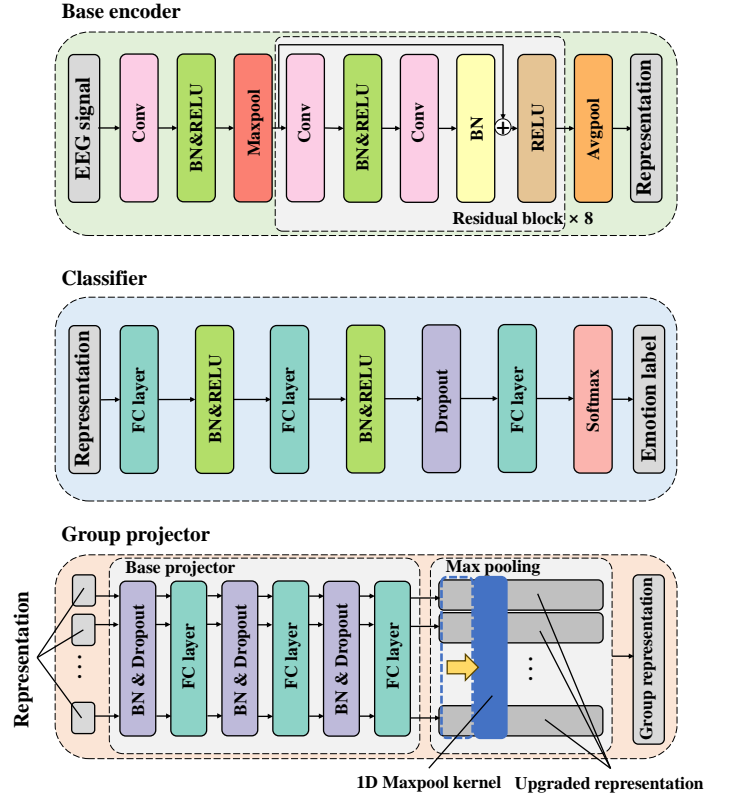


Fig. 4. Details of the architecture of the base encoder, group projector, and classifier. *Conv* represent convolutional layer with 1D kernel. *Maxpool* and *Avgpool* represent Max pooling and Avg pooling with 1D kernel. *BN* represent Batch Normalization. *FC* layer represent fully-connected layer. *RELU* represent Rectified Linear Unit.

Inspired by it, we adopted a symmetric function to design a model suitable for extracting features from group EEG signals. As illustrated in Fig.4 we designed the group projector consisting of a base projector and symmetric function MaxPool1D.

To mitigate individual feature loss, the dimension of individual representation can be upgraded for extraction. We introduce the base projector  $l: \mathbb{R}^D \rightarrow \mathbb{R}^H$  that adopt a multilayer perceptron (MLP) to project each individual representation  $\mathbf{h}$  on a 4096-dimensional feature space. The base projector contains three fully-connected layers with 1024, 2048, and 4096 hidden units in ascending order and adopt ReLU as the activation function of the first two layers. Batch Normalization and Dropout with 0.5 are shown in the corresponding positions in the figure.

To ensure an invariant output to represent the group sample with any input permutations, 1-dimension max-pooling (Max-Pool1D) is adopted to aggregate the information from each dimension-upgraded representation. As illustrated in Fig.4, the 1D kernel of MaxPool1D is perpendicular to the dimension-upgraded representation vector. The scanning direction of the kernel is parallel to upgraded representation vector with a stride of 1, and the padding is 0. Such MaxPool can extract the maximum values on 4096 feature dimensions from  $Q$  dimension-upgraded representations to obtain the group-level

feature representation in latent space.

We note group projector as  $g : \mathbb{R}^{Q \times D} \rightarrow \mathbb{R}^H$ . Extracted group representation in latent space can be obtained through  $g$  as follows:

$$z_v^t = g(\mathbf{H}_v^t) = \text{MaxPool1D}(l(\mathbf{h}_1), l(\mathbf{h}_2), \dots, l(\mathbf{h}_Q)) \quad (5)$$

#### F. Classifier

In the emotion classification fine-tuning task, we use the classifier to extract emotional features and predict emotion labels from the representations extracted by the base encoder. As illustrated in Fig.4 the classifier mainly contains three fully-connected layers with 512, 256, and 128 hidden units in descending order. Batch Normalization ReLU and Dropout with 0.5 are shown in the corresponding positions in the figure.

#### G. The Contrastive Loss

To measure the similarity of group-level stimuli-related features between two group samples, we can calculate the cosine similarity of their group representation vectors. The input group samples  $\{\tilde{\mathbf{G}}_i^t | i = 1, 2, \dots, P; t \in \{A, B\}\}$  would be extracted to obtain group feature representations  $\{z_i^t | i = 1, 2, \dots, P; t \in \{A, B\}\}$  via the base encoder and group projector. Then, the similarity of two augmented group samples  $\tilde{\mathbf{G}}_i^A$  and  $\tilde{\mathbf{G}}_j^B$  can be calculated on  $z_i^A$  and  $z_j^B$ :

$$s(z_i^A, z_j^B) = \frac{z_i^A \cdot z_j^B}{\|z_i^A\| \|z_j^B\|}, s(z_i^A, z_j^B) \in [0, 1] \quad (6)$$

The contrastive loss is designed to maximize the similarity of two group-level representations of groups sharing the same stimuli label in a positive pair. Similar to the SimCLR framework [38], we adopt the normalized temperature-scaled cross-entropy to define loss function as follows:

$$\ell_i^A = -\log \frac{\exp(s(z_i^A, z_j^B)/\tau)}{\sum_{j=1}^P \mathbb{1}_{[j \neq i]} \exp(s(z_i^A, z_j^A)/\tau) + \sum_{j=1}^P \exp(s(z_i^A, z_j^B)/\tau)} \quad (7)$$

where  $\mathbb{1}_{[j \neq i]} \in \{0, 1\}$  is an indicator function equaling to 1 if  $j \neq i$ .  $\tau$  is the temperature parameter of softmax. The smaller the loss function is, the larger similarity between  $z_i^A$  and  $z_j^B$ , and the smaller the similarity between  $z_i^A$  and other group representations come from the same minibatch.

Finally, the total loss for an iteration is the average of all contrastive losses for backpropagation as follows:

$$\mathcal{L} = \frac{1}{2P} \sum_{i=1}^P (\ell_i^A + \ell_i^B) \quad (8)$$

#### H. Pre-training Process

Based on the constructed group sampler, data augmentation, base encoder, group projector, and loss function the SGMC pre-training can be performed.

In a pre-training, we first set a number of epochs  $T_1$ , and then iterate the epoch. In each epoch, we continue to sample  $P$  video clips per iteration until all video clips are enumerated. Each iteration, Sampler extract  $2PQ$  EEG samples  $\mathcal{D} = \{\mathbf{X}_{v_i}^{s_k} | i = 1, 2, \dots, P; k = 1, 2, \dots, 2Q\}$  and pack them into groups  $\mathcal{G} = \{\mathbf{G}_i | i = 1, 2, \dots, P\}$ .

Nextly for the Meiosis data augmentation, to avoid the model cheating by recognizing the split position, we randomly generate a fixed split position  $c$ , sent it to each time of Meiosis in this iteration ( $1 < c < M - 1$ ).  $2Q$  augmented group samples  $\tilde{\mathcal{G}} = \{\tilde{\mathbf{G}}_i^t | i = 1, 2, \dots, P; t \in \{A, B\}\}$  can be obtained by (3). Further we extract group-level features and project them to latent space to obtain group representations by (4) and (5). Furthermore, we calculate loss  $\mathcal{L}$  by (6)-(8). Finally, we abate loss  $\mathcal{L}$  by backpropagation to calculate the gradient for optimizer updating parameters of  $f$  and  $g$ . Detailed procedures are summarized in Algorithm 1.

---

#### Algorithm 1 Self-supervised Group Meiosis Contrastive Learning

---

**Input:** Number of video clips  $P$  per minibatch, number of subjects  $Q$  per group. Initialized base encoder  $f$  and group projector  $g$ .

- 1: **for** *epoch* = 1 to  $T_1$  **do**
  - 2:   **repeat**
  - 3:     Sample  $P$  video clips  $\{v_i | i = 1, 2, \dots, P\}$ .
  - 4:     Randomly select  $2Q$  subjects  $\{s_k | k = 1, 2, \dots, 2Q\}$ .
  - 5:     Sampler pack minibatch  $\mathcal{G} = \{\mathbf{G}_i | i = 1, 2, \dots, P\}$  from  $\mathcal{D} = \{\mathbf{X}_{v_i}^{s_k} | i = 1, 2, \dots, P; k = 1, 2, \dots, 2Q\}$
  - 6:     Randomly generate a split position  $c$ .
  - 7:     Obtain  $\tilde{\mathcal{G}} = \{\tilde{\mathbf{G}}_i^t | i = 1, 2, \dots, P; t \in \{A, B\}\}$  from  $\mathcal{G}$  through Meiosis with  $c$  by (1)-(3).
  - 8:     Obtain  $\mathcal{Z} = \{z_i^t | i = 1, 2, \dots, P; t \in \{A, B\}\}$  from  $\tilde{\mathcal{G}}$  through  $f$  and  $g$  by (4) and (5).
  - 9:     Calculate loss  $\mathcal{L}$  by (6)-(8).
  - 10:    Abate loss  $\mathcal{L}$  through optimizer updating parameters of  $f$  and  $g$ .
  - 11:   **until** all video clips are enumerated.
  - 12: **end for**
- Output:** base encoder  $f$ , throw away group projector  $g$ .
- 

#### I. Fine-tuning Process

To achieve excellent emotional classification performance, based on learned feature representations we further fine-tune the model with labeled samples. As illustrated in Fig.1 emotion classification supervised training is performed on the model consisting of an initialized classifier and the SGMC pre-trained base encoder.

We denote the training data as  $\mathbf{X}$  and their labels as  $\mathbf{y}$ . We denote the classifier as  $k(\cdot)$ . The label  $\mathbf{y}$  is a categorical variable. For example, if there are four emotional categories,  $\mathbf{y}$  can take four values: 0, 1, 2 or 3. We need to predict the emotion category  $\mathbf{y}$  for each sample  $\mathbf{X} \in \mathbb{R}^{M \times C}$ . The pre-trained base encoder  $f$  extracts the representation from original EEG signal  $\mathbf{X}$  for classifier  $k(\cdot)$  extract predictive features to obtain prediction category  $\mathbf{y}^{pre} = k(f(\mathbf{X}))$ . We apply the cross entropy function to define the loss function for the emotion classification task and apply an optimizer to minimize the loss function to optimize the parameters of the model. Finally, when the loss function converges, a predictive EEG-based emotion recognition model is obtained.

## IV. EXPERIMENTS

In this section, we introduce the implementation detail on the DEAP and SEED dataset and our experiment evaluation. In our experiment, we verify the effectiveness by comparing the SGMC with other competitive methods of emotion recognition and evaluating its performance on limited labeled sample learning. Further, we explore the reason for the effectiveness by visualizing the feature representation learned by the SGMC. Moreover, we explore the meaningful law of the framework by evaluating the different combinations of hyper parameters. Furthermore, we verify the rationality of architecture design by conducting control and ablation experiments.

### A. Implementation Detail

In this section, we elaborate on our implementation detail of the dataset, data processing, and basic hyper parameters utilized in the experiments.

#### (1) Dataset

**DEAP:** The widely-used DEAP dataset [21] includes 32-channel EEG signals and 8-channel peripheral physiological signals recorded by 32 subjects when watched 40 pieces of a one-minute music video. Each trial data was recorded under 3-seconds of resting state and 60-seconds of stimuli. The recorded EEG signals are down-sampled to a 128 Hz sampling rate and processed with a bandpass frequency filter from 4-45 Hz by the provider. After watching each video, subjects were asked to rate their emotional levels of arousal, valence, liking, and dominance from 1 to 9 for each video. We adopt the EEG signals and rating values of arousal and valence to perform emotion recognition. We set the threshold value of the rating value of arousal and valence at 5. When the rating value is more than 5.0, the corresponding EEG signals are labeled as high arousal or valence. Otherwise, it is labeled as low arousal or valence. Each EEG signal corresponds to valence and arousal two labels, which can be used to construct two or four classification tasks.

**SEED:** The SEED dataset is widely used in emotion recognition algorithms [39]. The dataset recorded the EEG signals from 15 subjects when watching 15 videos selected from movies in three categories of emotions, including positive,

neutral, and negative. Each video is about 4 minutes long. Each subject repeated the experiments for three sessions, with an interval of more than one week. The EEG signals were recorded via 62 electrodes at a sampling rate of 1000Hz and have been downsampled to 200 Hz and filtered from 0 to 75 Hz by the provider.

#### (2) Data Process

On the DEAP, we use a 1-second-long sliding window to separate the 63s signal of each trial into 63 non-overlapping EEG signal segments. To improve accuracy, following existing work [28] we reduce the 3s resting state EEG signals from the 60s emotional stimuli EEG signal. In detail, in each trial, we average the 3s baseline EEG signal segments to get a 1s average baseline EEG signal segment. The remaining 60 segments each subtract the average baseline segment to become input samples. All samples correspond to a total of 2400 (40 videos with 60-seconds-long) repeated 1-second-long video clips. 1680, 320, and 320 1-second video clips are randomly divided into three sets from 2400 video clips in the ratio of 70:15:15. These three sets of video clips that were watched by 32 subjects correspond to 53760, 11520, and 11520 (70:15:15) EEG segments which are used as the training set, testing set, and validation set respectively.

On SEED, we first perform an L2 normalization for each trial of EEG signal in each channel. Similar to the DEAP dataset we divide movie videos into 1-second windows. Because the length between the trial videos is different, we segment adjacent windows from front to back according to the time axis until the coverage of windows exceeds the video range. 3394 video clips are obtained from 15 movie videos and randomly divided into 2734, 510, and 510 clips, which three sets of video clips are in the ratio of 70:15:15. These three sets of video clips that were watched by 15 subjects three times correspond to 123030, 22950, and 22950 (70:15:15) EEG segments which are used as the training set, testing set, and validation set respectively.

#### (3) Basic Configuration

To accurately evaluate the performance of emotion recognition for a pre-training framework, there are two steps we adopted for evaluating the results. We first save pre-trained models with the different epochs. Next, we select the model with the highest average accuracy on emotion recognition

TABLE I  
HYPER PARAMETERS UTILIZED IN THE PROPOSED SGMC

		$Epoch$	$batchsize$	$lr$	$\tau$	$P$	$Q$	$Shape_{tr}$	$Shape_{te}/Shape_{val}$
DEAP	Pre-training	2800	32	$10^{-4}$	$10^{-1}$	8	2	(1680, 32, 1, 32, 128)	(360, 32, 1, 32, 128)
	Fine-tuning	60	2048	$10^{-3}$	-	-	-	(53760, 1, 32, 128)	(11520, 1, 32, 128)
SEED	Pre-training	3288	64	$10^{-3}$	$10^{-1}$	16	2	(2374, 45, 1, 62, 200)	(510, 45, 1, 62, 200)
	Fine-tuning	70	256	$10^{-3}$	-	-	-	(106380, 1, 62, 200)	(22950, 1, 62, 200)

$Shape_{tr}$ ,  $Shape_{te}$ ,  $Shape_{val}$  respectively represent size of tensor of training test and validation dataset for pre-training or fine-tuning.  $Epoch$  represent an appropriate number of the pre-training or fine-tuning epochs for achieving the fine emotion recognition performance.  $batchsize$  represent the number of samples in a minibatch.

obtained by five times of fine-tuning. Such average accuracy is evaluated as the result.

To speed up sampling, in the pre-training process we set the five axes of dataset tensor to correspond to *video clip*, *subject*, 1, *channel*, *sampling point* respectively. In the fine-tuning process, the first two axes *video clip* and *subject* of the dataset are reshaped into a sample axis. Each axis of reshaped dataset corresponds to *sample*, 1, *channel*, *sampling point* in turn. In the pre-training task, each epoch traverses every video clip of the dataset, a fine pre-training task generally needs to train more than 2000 epochs. To reduce the workload, we use the validation dataset to adjust the hyper parameters of the SGMC framework and use the test dataset to evaluate the model. The tensor shape of the training set, testing set, and validation set are represented as  $Shape_{tr}$ ,  $Shape_{te}$ , and  $Shape_{val}$  and are listed in Table I.

In this paper, we use PyTorch [40] to implement our experiments based on the NVIDIA RTX3060 GPU. The Adam optimizer [41] is used to minimize the loss functions for both the pre-training and fine-tuning process. We represent  $lr$  as the learning rate of the optimizer. In the pre-training process and fine-tuning process, the number of epochs, batch size, the temperature parameter  $\tau$ , learning rate  $lr$ , number of video clips per iteration  $P$ , number of samples per group  $Q$ , and size of the tensor of the dataset have applied different values, as shown in Table I, we list all hyper parameters utilized in two processes on DEAP and SEED dataset.

## B. Emotion Classification Performance

### (1) Performance on DEAP

As illustrated in Table II, On the DEAP dataset, We first compare the SGMC with four state-of-the-art methods in the two emotion dimensions of valence and arousal: one residual long short-term memory network utilizing multi-modal data MMResLSTM [43], a channel-fused dense convolutional network CDCN [42], and a hybrid network of convolutional neural networks and recurrent networks with a channel-wise attention mechanism ACRNN [44]. From Table II, it can be found that the accuracy of the proposed SGMC is 1% higher than the second in the valence dimension and 2.3% higher than in the arousal dimension. The comparison results demonstrate the effectiveness of the SGMC on EEG-based emotion recognition.

To verify the effectiveness of the proposed framework in the data augmentation and self-supervised learning fields, we further compare the SGMC with a GAN-based data augmentation method MCLFS-GAN [45] and a self-supervised GAN-based data augmentation framework GANSER [36]. Especially, according to the experimental setting of MCLFS-GAN [45] and GANSER [36], we further perform a comparison on a four-category classification problem: distinguishing EEG signals of four categories: high valence and high arousal, high valence and low arousal, low valence and high arousal, and low valence and high arousal. In Table II, it can be found that the proposed method outperforms the existing data augmentation and self-supervised learning method over 11.33% and 2.09% on four-

TABLE II  
PERFORMANCES ON DEAP

Method	Valence	Arousal	Four
CNN-LSTM (2020) [28]	90.82	86.13	-
CDCN (2020) [42]	92.24	92.92	-
MMResLSTM (2019) [43]	92.87	92.30	-
ARCNN (2019) [44]	93.72	93.38	-
MCLFS-GAN (2020) [45]	-	-	81.32
GANSER (2022) [36]	93.52	94.21	89.74
Proposed(Fully-supervised)	91.23	92.36	87.68
Proposed(Fine-tuned)	<b>94.72</b>	<b>95.68</b>	<b>92.65</b>

Average accuracy(%) of state-of-the-art method on the DEAP dataset for valence classification, arousal classification and four classification.

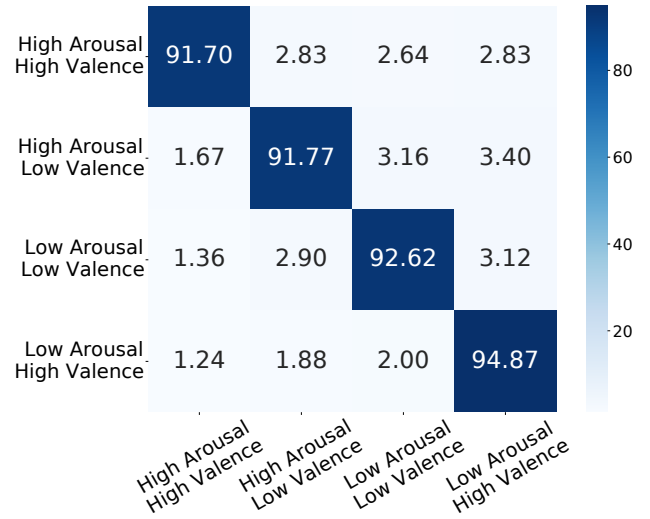


Fig. 5. The confusion matrix of classification on DEAP

category classification. As illustrated in Fig.5. meanwhile, the confusion matrices of the SGMC on four-category classification are presented. It shows that the SGMC achieves good performance in each category, especially in low arousal and high valence.

Furthermore, we first compare the proposed SGMC with our own fully-supervised baseline using the same network model without pre-training. In valence, arousal, and four-category dimensions, the accuracy of the SGMC exceeds the fully-supervised baseline over 3.49% 3.32% and 4.97%, which shows the significant effect of improving emotion recognition.

### (2) Performance on SEED

As illustrated in Table III, Similar to the DEAP, we first compare our proposed SGMC with four fully-supervised state-of-the-art studies : GRSLR [46] adopting a graph regularized sparse linear regression model, BiHDM [24] utilizing two independent recurrent networks for the left and right hemispheres of the brain, DGCNN [47] adopting a dynamic graph convolutional neural network, and a 1D CNN-based residual neural network ResNet18 [29]. Results use accuracy in the

TABLE III  
PERFORMANCES ON SEED

Method	Accuracy(%)			
	1%	10%	50%	100%
GRSLR(2018) [46]	-	-	-	87.39
DGCNN(2018) [47]	-	-	-	90.40
BiHDM(2019) [24]	-	-	-	93.12
ResNet18 1D kernel(2021) [29]	-	-	-	93.43
Proposed(Fully-supervised)	44.81	59.77	85.47	89.83
Proposed(Fine-tuned)	<b>89.65</b>	<b>93.29</b>	<b>93.71</b>	<b>94.04</b>

Average accuracy(%) of state-of-the-art method on the SEED dataset for positive, neutral and negative three-classification. Percentages of labels represent labeled samples use to training emotion recognition account for the percentage of the full training set.

three classification tasks of positive neutral, and negative emotions. As illustrated in Fig.5. The details of the classification result are shown in the confusion matrix. The SGMC achieves good accuracy in three categories, especially performing better on positive than negative and neutral. As illustrated in Table III the proposed SGMC outperforms the four state-of-the-art studies, reflecting its good emotion recognition performance on the SEED.

Further, we compare the SGMC with our fully-supervised baseline using the same model. Especially, the SEED dataset has nearly five times the data volume of the DEAP dataset. Therefore, it can better reflect the performance of self-supervised learning by utilizing a large number of unlabeled samples to make up for scarce artificial accurate labels. We report results obtained from fine-tuning with four various percentages of the total training set labeled samples (based on pre-training on the full training set). From 1% to 50% percentage of labeled samples, the SGMC exceeds our fully-supervised baseline over 44.84%, 33.52%, and 8.24%. Such results show the proposed SGMC can take advantage of consistency of stimuli to significantly make up for artificial accurate labels. Using the full training set labeled samples to fine-tune, the SGMC significantly exceed our fully-supervised baseline over 4.27% as well. This shows the SGMC contributes a significant improvement by utilizing large unlabeled data.

### C. Performance on Limited Labeled Sample Learning

Based on the above results on SEED, it can be found that fewer labeled samples can also lead to good results. To evaluate the performance on limited labeled sample learning, we further evaluate the results on DEAP and SEED when the number of labeled samples per category increasing. We adopte a model based on SGMC pre-trained with the full training set and an initialized model to compare their performance on fine-tuning/fully-supervised learning with the same limited labeled sample. On the DEAP the results adopt a four-category

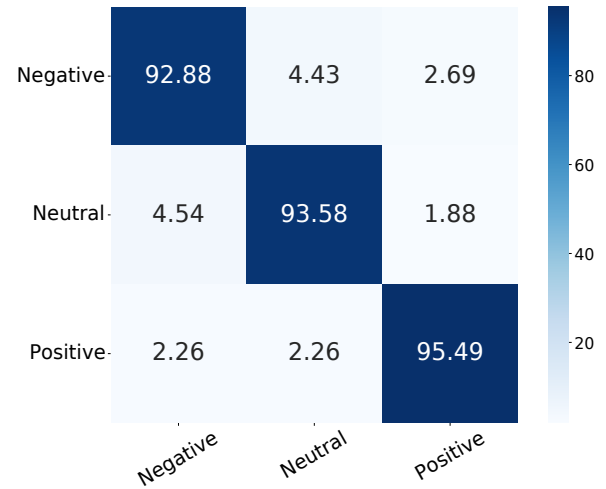


Fig. 6. The confusion matrix of classification on SEED

classification of arousal and valence. On SEED the results adopt a three-category classification. As illustrated in Fig. 7. the results of the different number of labeled samples per category for fine-tuning/fully-supervised learning are reported.

we can find that in any amount of labeled samples regimes, the accuracy of the SGMC fine-tuning is significantly superior to the fully-supervised baseline, and it is more significant in the lower labeled samples regime. On the DEAP dataset, when the number of labeled samples per category is over 10, the performance of the SGMC significantly outperforms the supervised. When fine-tuned with 5000 labeled samples per category (37.2% of the full training set), the SGMC reaches a good accuracy of 87.51% which is nearly by 87.68% of fully-supervised accuracy training with the full training set. On the SEED dataset, when fine-tuned with even only one labeled sample per category (0.00278% of the training set), the SGMC reached an accuracy of 59.42%. When fine-tuned with 50 samples per category (0.14% of the training set), the accuracy of 91.01% outperforms the fully-supervised baseline with 100% labeled data. Further, we observe that when the number of category is over 500, the curve has converged. This shows the SGMC enables a significant decline in the demand for artificial labels and reflects the consistency of stimuli have been well exploited to make up for artificial labels.

### D. Representation Visualization

To explore how SGMC contributes to superior performance on emotion recognition, we visualize the learned feature representations of the SGMC fine-tuned model and the only fully-supervised model.

As illustrated in Fig. 8, the 512-dimension feature representations extracted by the base encoder from the samples of the full SEED testing set are projected to two dimensions through t-SNE [48]. In the figure above, 15 colors represent samples corresponding to the 15 trial video clips (about 4-minutes). It can be found that in the visualization of the SGMC fine-tuned (right), the feature representation of the same video clip

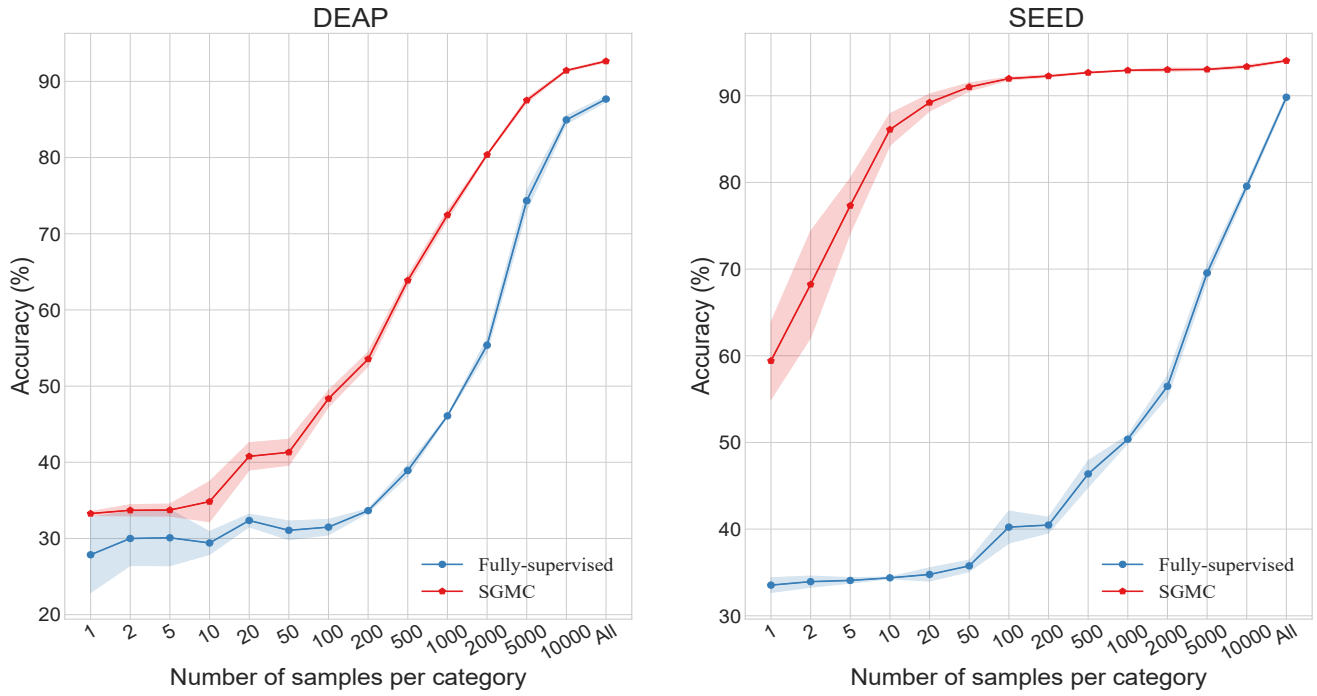


Fig. 7. Learning effect of the labeled sample size for the emotion recognition. the left is for the result on DEAP, and the right is for SEED. The red line represents the model is based on the SGMC pre-trained with the full training set and fine-tuned with the different number of labeled samples per category. Blue line represents the model is only fully-supervised trained with the different number of labeled samples per category. The results are the average accuracy of five times of emotion classification training and the shade area represents standard deviation.

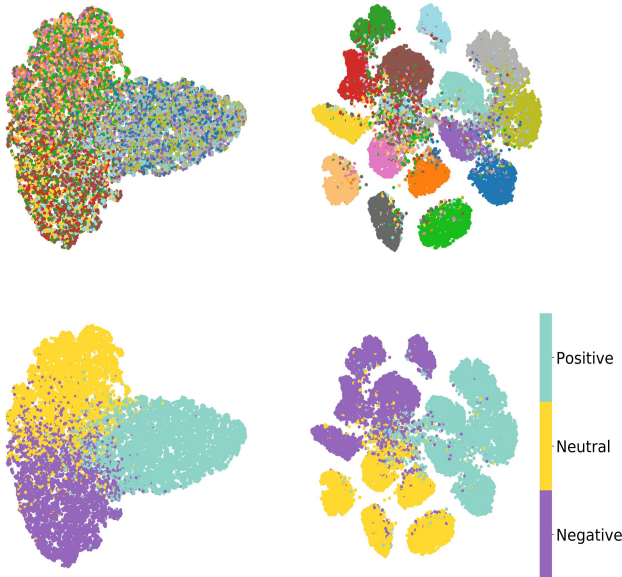


Fig. 8. t-SNE visualization for feature representations demonstrated on SEED with fully-supervised (left) and the SGMC fine-tuned (right). Tops are the visualization marked by movie videos, and the different colors represent the 15 videos. Bottoms are the visualization marked by emotion labels, and three colors represent positive, neutral, and negative videos respectively.

tends to gather together to form 15 distinguishable groups. On the contrary, in the visualization of fully-supervised (left), the representations corresponding to the different video clips cannot be distinguished significantly. Visualization reveals that the

SGMC not only learns stimuli-related feature representations but also enables the model to distinguish whether different stimuli come from a continuous video. Further, we mark the corresponding emotion labels with three colors in the figure below. There are more indistinguishable representations with different emotion labels mixed together in fully-supervised visualization (left). In the SGMC fine-tuned visualization (right), there are fewer feature representations with the different emotion labels mixed together and shows better emotional discrimination. It reflects that the SGMC enables the model to learn the video-level stimuli-related representation to improve emotion recognition performance.

### E. Effect of Hyper Parameters

To explore the effect of the number of samples per group ( $Q$ ) and the number of selected video clips per iteration ( $P$ ) on contrastive learning, we evaluate various combinations of hyper parameters. In our experiment strategy, each given  $Q$ , we evaluate various  $P$  including 2, 4, 8, 16, 32, 64, and select the one that achieves the best result on emotion recognition as the appropriate  $P$  for given  $Q$ . The results of the different  $Q$  on emotion recognition are illustrated in Fig.11. The appropriate  $P$  and number of epochs of pre-training, and corresponding pre-training accuracy of the different  $Q$  are reported in Table IV .

On the DEAP, When  $Q = 2$  and  $P = 4$ , the SGMC achieves the best performance. On the SEED, when  $Q = 2$  and  $P = 16$ , the SGMC achieves the best performance.

TABLE IV  
ILLUSTRATION OF THE APPROPRIATE COMBINATION OF HYPER  
PARAMETERS OF  $Q$  AND  $P$  IN THE HYPER PARAMETER ANALYSIS ON  
DEAP AND SEED.

DEAP				SEED			
Q	P	$Epoch_{pre}$	$acc_{pre}$	Q	P	$Epoch_{pre}$	$acc_{pre}$
1	16	440	70.56	1	8	1992	71.58
2	8	2800	91.11	2	16	3288	80.68
3	8	3600	87.50	3	32	1296	66.24
4	4	800	93.06	4	32	744	69.82
8	4	475	96.94	7	32	548	72.45
16	4	450	97.08				

$Epoch_{pre}$  represent the appropriate number of epochs of pre-training,  $acc_{pre}$  represent the accuracy of pre-training task,  $Q$  represent number of samples per group,  $P$  represent number of sampled video clips per iteration.

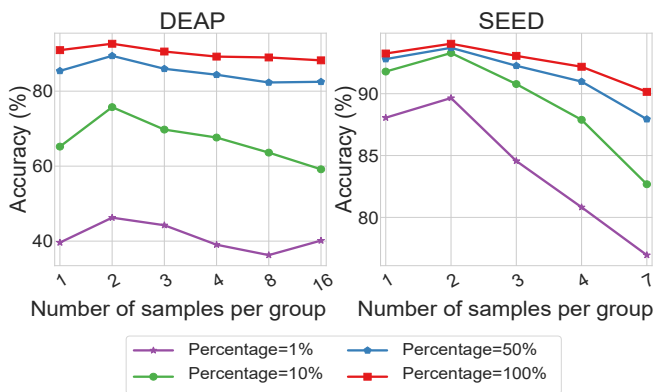


Fig. 9. The group size effect on accuracy of DEAP (left) and SEED (right). The x-axis represents the number of samples ( $Q$ ). The four lines with colors show the various percentage of labeled samples used for fine-tuning in the training set.

Further, it can be observed that an opposite law exists in the DEAP and SEED datasets. When given a larger  $Q$ , the appropriate  $P$  on the DEAP tends to be smaller, and on the SEED tends to be larger. The possible reason is the difference in labeling between the two datasets. On the SEED, the emotional labels are labeled by the experiment designer, which is determined by the emotional attribute of the video stimuli. On the DEAP dataset, emotional labels are labeled by the rating of the subjects. Such labeling is more related to the personalized differences of the subject than to the SEED. And because the larger  $P$ , the more difficult the contrastive learning is. At the time the model is more encouraged to focus on extracting stimuli-related features and ignore the personalized features that are irrelevant stimuli. So the larger  $P$  lead to better results on the SEED and hinders better results on the DEAP. This indicates that a smaller  $P$  should be considered first to use when the data was labeled by the subject, and a larger  $P$  should be considered first to use when the data was labeled by the emotional attributes of the stimuli.

Furthermore, it can be found that generally the greater the  $Q$  (when  $P$  are constant), the greater the accuracy of pre-

TABLE V  
ILLUSTRATION OF APPROPRIATE NUMBER OF EPOCHS OF THE  
PRE-TRAINING ON DEAP AND SEED WHEN COMPARING THE SYMMETRIC  
FUNCTIONS.

Symmetric function	$Epoch_{pre}$	
	DEAP	SEED
MinPool1D	2440	1480
AvePool1D	1720	2472
MaxPool1D	2880	3288

training. The possible reason is that the greater group sample contains the more comprehensive group-level stimuli-related features to alleviate the interference of random distractions, fatigue, and individual differences. However, good accuracy in pre-training is not always beneficial to emotion recognition. Too smaller  $Q$  leads to lower accuracy of pre-training, which hinders the learning of meaningful representation. Too larger  $Q$  leads the model to focus on the aggregation of group-level stimuli-related features and leads the base encoder to ignore learning some emotion-related features to hinder better emotion recognition. So it is critical to select an appropriate  $Q$  for constructing the group-sample-based contrastive learning.

#### F. Architecture Design Analysis

In this section, we validate our designed choices by control and ablation experiments. We first verify the rationality of the symmetric function we choose. Furthermore, we evaluate the rationality of the strategy of constructing the group sample, utilizing Meiosis augmentation, and constructing the positive-negative pairs.

##### (1) Comparison with Various Symmetric Function

The SGMC selects the symmetric function MaxPool1D to construct the group projector. To verify its rationality, we compare MaxPool1D with a common similar AvgPool1D and an additional opposite MinPool1D which is implemented by taking the minimum value in each dimension of upgraded representations. Illustrate in Fig.4. and Table IV MaxPool1D is significantly better than others. The possible reason is that MaxPool1D is more beneficial for model selecting emotion-related features to extract from upgraded feature representations. Although MinPool1D also has a selection ability, the features it selects are more detrimental to improving learning emotion-related representation. This verifies the rationality of using MaxPool1D to aggregating group features for contrastive learning.

##### (2) Ablation Study

To investigate the rationality of some novel designs of the architecture, we conduct an ablation study for these three components: group sample, Meiosis data augmentation, and stimuli consistency. We can get the new version by removing one or two components, and the evaluation strategy is consistent with the basic configuration. When the group sample is ablated, we use individual samples for contrastive learning (just let  $Q = 1$ ). When Meiosis data augmentation

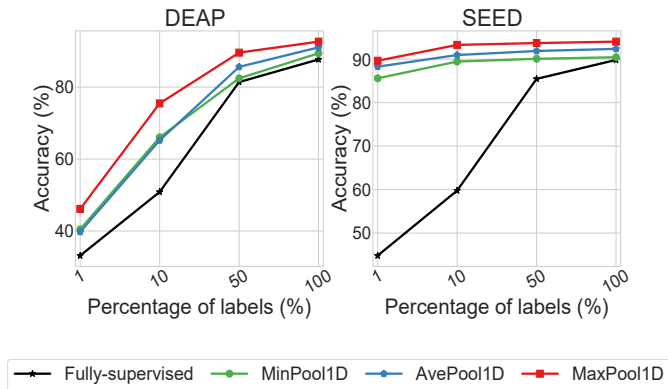


Fig. 10. Emotion classification accuracy based on fully-supervised model and SGMC fine-tuned model with various symmetric functions on DEAP (left) and SEED (right). The x-axis represents the percentages of labeled sample for fine-tuning/supervised training in the training set.

TABLE VI

THE COMPONENTS OF THE FIVE NEW VERSIONS AND THE COMPLETE SGMC, AND THE APPROPRIATE NUMBER OF EPOCHS FOR PRE-TRAINING WITH EACH VERSION ON DEAP AND SEED.

Method	Group	Augment	Consistent	$Epoch_{pre}$	
				DEAP	SEED
Non-group	✗	Crossover	✓	440	1848
Non-augment	✓	No augment	✓	800	2280
Mixup-augment	✓	Mixup	✓	275	1304
Non-consistent	✓	Crossover	✗	60	2752*
Consistent-only	✗	No augment	✓	1740	2368
Proposed	✓	Crossover	✓	2800	3288

\* Non-consistent leads to worse performance of emotion recognition than fully-supervised on the SEED dataset, so we adopt the result obtained when the loss function of pre-training converges.

$Epoch_{pre}$  represents the appropriate number of epochs of pre-training.

No augmet represent ablating crossover, Crossover represent adopt crossover to data augment ,and Mixup represent adopt Mixup to substitute crossover

is ablated, for augmenting the group/individual samples we skip the crossover process and go directly into the separation process after completing individual pairing. After removing the stimuli consistency, we change the way of constructing the positive pair with samples sharing the same stimuli. Instead, the sampler is required randomly sample EEG signals with any stimuli to form the sample group for augmenting and constructing pairs.

The results of the four-category classification on DEAP and three-category classification on SEED are reported in Fig.11. The detail of ablation and the number of epochs of pre-training are reported in Table VI.

To verify the effectiveness of group sample on the SGMC, we design a version Non-group by removing the group sample. It can be observed that the emotion recognition performance significantly declined on DEAP and SEED by more than

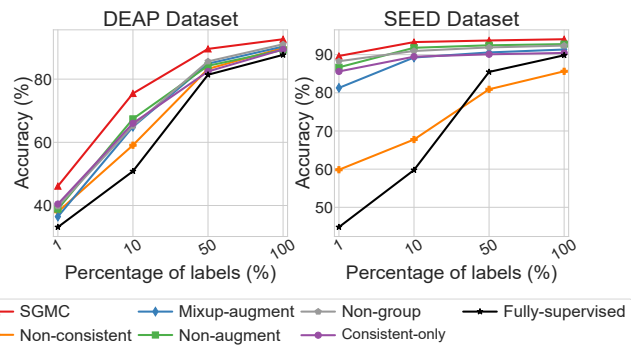


Fig. 11. Emotion classification accuracy based on the five new versions fully-supervised, and the complete SGMC on DEAP (left) and SEED (right). The x-axis represents the percentages of labeled sample for fine-tuning/supervised training in the training set.

1.5%. This reflects group sample is important to alleviate the obstacles of contrastive learning for the SGMC framework. To verify the effectiveness of Meiosis augmentation, we design a version Non-augment by removing Meiosis augmentation. It can be observed that on DEAP the accuracy decreases significantly more than 3%, and on SEED decreases by more than 1.2%. It verifies the critical role of Meiosis data augmentation to improve emotion recognition in the SGMC. To verify the superiority of Meiosis utilizing the stimuli alignment in the group sample, we design a competitive version Mixup-augment. For the mutual augmentation of two samples, we can naturally think of Mixup [49] data augmentation, which can mix two samples and generate two samples. We construct the Mixup-augment version by substituting the crossover of Meiosis with Mixup. The result shows the Meiosis-based SGMC significantly exceeds Mixup-augment by more than 2.3% on the DEAP and 2.6% on SEED. This shows the effectiveness of designing the Meiosis data augmentation by mimicking the physiological mechanisms of meiosis. To verify the importance of constructing the positive-negative pair based on the consistent stimuli, we design a version Non-aligned by removing stimuli consistent. The results significantly decrease by more than 2.7% on DEAP, even lower than the fully-supervised baseline on SEED. It reflects that stimuli consistent is critical to guiding learning meaningful stimuli-related feature representation by constructing instructive positive-negative pairs. Further, to investigate the utilizability of potential stimuli consistency, we perform a version Consistent-only by removing the group sample and Meiosis augment, and keeping stimuli consistent only for contrastive learning. The result exceeds the fully-supervised baseline by more than 1.7% on DEAP and by more than 0.6% on SEED, which indicates that consistency of stimuli are exploitable but hindered.

## CONCLUSION AND FUTURE WORK

In this work, a self-supervised Group Meiosis Contrastive learning (SGMC) framework is designed to improve emotion recognition. In the proposed framework, Meiosis data

augmentation is introduced to augment EEG group samples without changing stimuli features. A base encoder and a group projector are designed in the model to extract group-level feature representations. With the consistency of stimuli, contrastive learning is designed to learn stimuli-related feature representation.

The proposed framework achieves state-of-the-art emotion recognition results on the DEAP, and also reaches competitive performance on the SEED datasets. Compared to the fully-supervised baseline, the SGMCI improves emotion recognition significantly, especially when there are limited labels. In addition, the results of feature visualization suggest that the model might have learned the video-level feature representations, and improves the performance of the model. The hyper parametric analysis further demonstrates the role of group samples during emotion recognition. Finally, the rationality of the framework design including the selection of symmetric functions, the construction of the positive-negative pairs, and Meiosis data augmentation are verified.

In the future, we will continue to develop such kinds of group-sample-based SSL frameworks while with low calculation costs.

#### REFERENCES

- [1] U. Cowie, E. Douglas-Cowie, N. Tsapatsoulis, G. Votsis, S. Kollias, W. Fellenz, and J. G. Taylor, "Emotion recognition in human-computer interaction", *IEEE Signal processing magazine*, vol. 18, no. 1, pp. 32–80, 2001.
- [2] I. Ariely and G. S. Berns, "Neuromarketing: the hope and hype of neuroimaging in business", *Nature reviews neuroscience*, vol. 11, no. 4, pp. 284–292, 2010.
- [3] D. Song, W. Zheng, P. Song, and Z. Cui, "EEG emotion recognition using dynamical graph convolutional neural networks," *Trans. Affective Computing*, 2020, vol. 11, no. 3, pp. 532–541.
- [4] E. Du, C. Ma, G. Zhang, J. Li, Y.-K. Lai, G. Zhao, X. Deng, Y.-J. Liu, and H. Wang, "An efficient LSTM network for emotion recognition from multichannel EEG signals," *Trans. Affective Computing*, pp. 1–1, 2020.
- [5] Y. Tao, C. Li, R. Song, J. Cheng, Y. Liu, F. Wan, and X. Chen, "EEG-based emotion recognition via channel-wise attention and self attention" , *Trans. Affective Computing*, 2020, pp. 1–1.
- [6] F. Becker, J. Fleureau, P. Guillotel, F. Wendling, I. Merlet, and L. Al bera, "Emotion recognition based on high-resolution EEG recordings and reconstructed brain sources" , *Trans. Affective Computing*, vol. 11, no.2, 2020, pp. 244–257.
- [7] H. Zhang, M. Yu, Y.-J. Liu, G. Zhao, D. Zhang, and W. Zheng, "SparseDGCNN: Recognizing emotion from multichannel EEG signals" , *Trans. Affective Computing*, 2021, pp. 1–1.
- [8] I. Ye Z, Xie X, Y Liu, et al, "Understanding Human Reading Comprehension with brain signals", arXiv preprint, arXiv: 2108.01360, 2021.
- [9] F. Alimardani. M , Hermans. A , Tinga. M, et al, "Assessment of Empathy in an Affective VR Environment using EEG Signals", arXiv preprint, arXiv: 2003.10886, 2020.
- [10] B. Giakoumis D , Tzovaras D , Moustakas K , et al, "Automatic Recognition of Boredom in Video Games Using Novel Biosignal Moment-Based Features", *Trans. Affective Computing*, 2011, pp. 119–133.
- [11] L. Kalaganis F P , Adamos D A , Laskaris N A . "Musical NeuroPicks: a consumer-grade BCI for on-demand music streaming services", *Neurocomputing*, 2017, pp. 65–75.
- [12] H. Pandey P , Swarnkar R , Kakaria S , et al. Understanding Consumer Preferences for Movie Trailers from EEG using Machine Learning, *Annual Conference of Cognitive Science* 2020.
- [13] P. Balasubramanian S , Gullapuram S S , Shukla A . "Engagement Estimation in Advertisement Videos with EEG", arXiv preprint arXiv:1812.03364, 2018.
- [14] J. Banville H , Chehab O , Hyvrinen A , et al, "Uncovering the structure of clinical EEG signals with self-supervised learning", *Journal of Neural Engineering*, 2021, 18(4): 046020 (22pp).
- [15] I. Jiang X , Zhao J , Du B , et al, "Self-supervised Contrastive Learning for EEG-based Sleep Staging", *International Joint Conference on Neural Networks*, 2021, pp. 1–8.
- [16] J. P. Dmochowski, M. A. Bezdek, B. P. Abelson, J. S. Johnson, E. H. Schumacher, and L. C. Parra, "Audience preferences are predicted by temporal reliability of neural processing", *Nature communications*, vol. 5, no. 1, pp. 1-9, 2014.
- [17] J. P. Dmochowski, S. Paul, D. Joao, and L. C. Parra, "Correlated Components of Ongoing EEG Point to Emotionally Laden Attention—A Possible Marker of Engagement?", *Frontiers in Human Neuroscience*, vol. 6, 2012.
- [18] H. Shen X , Liu X , Hu X , et al, "Contrastive Learning of Subject-Invariant EEG Representations for Cross-Subject Emotion Recognition", *Trans. Affective Computing*. 2022.
- [19] C. Sara, B.C, Buonomo, et al, "Disjunction of Homologous Chromosomes in Meiosis I Depends on Proteolytic Cleavage of the Meiotic Cohesin Rec8 by Separin", *Cell*, 2000, pp. 387–397.
- [20] D. Bahari, Fatemeh, and Amin Janghorbani. "Eeg-based emotion recognition using recurrence plot analysis and k nearest neighbor classifier", *20th Iranian Conference on Biomedical Engineering (ICBME)*. IEEE, 2013.
- [21] K. Koelstra, C. Muhl, M. Soleymani, J.-S. Lee, A. Yazdani, T. Ebrahimi, T. Pun, A. Nijholt, and I. Patras, "DEAP: A database for emotion analysis using physiological signals", *Trans. Affective Computing*, vol. 3, no. 1, pp. 18–31, 2011.
- [22] G. Wang, Xiao-Wei, Dan Nie, and Bao-Liang Lu. "EEG-based emotion recognition using frequency domain features and support vector machines", *International conference on neural information processing*. Springer, Berlin, Heidelberg, 2011.
- [23] G. Alhagry, Salma, Aly Aly Fahmy, and Reda A. El-Khoribi. "Emotion recognition based on EEG using LSTM recurrent neural network". *Emotion* 8.10 : 355-358, 2017.
- [24] B. Li, W. Zheng, L. Wang, Y. Zong, L. Qi, Z. Cui, T. Zhang, and T. Song, "A novel bi-hemispheric discrepancy model for eeg emotion recognition." *IEEE Transactions on Cognitive and Developmental Systems* 13.2 pp: 354–367. 2020.
- [25] Y. Li, D. Song, P. Zhang, G. Yu, Y. Hou, and B. Hu, "Emotion recognition from multi-channel EEG data through convolutional recurrent neural network" , *International Conference on Bioinformatics and Biomedicine*, 2016, pp. 352–359.
- [26] T. Tripathi, S.; Acharya, S.; Sharma, R.D.; Mittal, S.; Bhattacharya, S. "Using deep and convolutional neural networks for accurate emotion classification on DEAP dataset", *AAAI*, pp. 4746–4752. 2017.
- [27] X. Shawky, E, El-Khoribi R, Shoman M.A.I, et al, "EEG-Based Emotion Recognition using 3D Convolutional Neural Networks", *International Journal of Advanced Computer Science and Applications* 2018, pp.329–337.
- [28] G. Yang, Q. Wu, M. Qiu et al, "Emotion recognition from multi-channel EEG through parallel convolutional recurrent neural network" , *International Joint Conference on Neural Networks*, 2018, pp. 1–7.
- [29] K. Cheah K H , Nisar H , Yap V V , et al, "Optimizing Residual Networks and VGG for Classification of EEG Signals: Identifying Ideal Channels for Emotion Recognition", *Journal of Healthcare Engineering*, 2021, pp. 1–14.
- [30] I. Gidaris S , Singh P , Komodakis N , "Unsupervised Representation Learning by Predicting Image Rotations", *International Conference on Learning Representations (ICLR)*, 2018.
- [31] H. Sermanet P , Lynch C , Hsu J , et al, "Time-Contrastive Networks: Self-Supervised Learning from Video", *International Conference on Robotics and Automation (ICRA)*, 2017, pp. 1-11.
- [32] E. Mikolov, I. Sutskever, K. Chen, G. S. Corrado, and J. Dean, "Distributed representations of words and phrases and their compositionality", *Advances in neural information processing systems*, vol. 26, 2013 pp. 3111–3119.
- [33] C. Devlin J , Chang M W , Lee K , et al, "BERT: Pre-training of Deep Bidirectional Transformers for Language Understanding", *Association for Computational Linguistics* 2018, pp. 4171-4186.
- [34] J. Saeed, F. D. Salim, T. Ozelebi, and J. Lukkien, "Federated self-supervised learning of multisensor representations for embedded intelligence" , *IEEE Internet of Things Journal*, vol. 8, no. 2, 2020, pp. 1030–1040.
- [35] O. Sarkar and A. Etemad, "Self-supervised learning for ecg-based emotion recognition" , *International Conference on Acoustics, Speech and Signal Processing (ICASSP)*, 2020 pp. 3217–3221.

- [36] G. Zhang Z , Zhong S H , Liu Y . "GANSER: A Self-supervised Data Augmentation Framework for EEG-based Emotion Recognition".*Trans. Affective Computing*, pp. 1–1, 2022.
- [37] S. Qi C R , Su H , Mo K , et al, "PointNet: Deep Learning on Point Sets for 3D Classification and Segmentation", *Conference on Computer Vision and Pattern Recognition*, 2017, pp. 77–85.
- [38] M. Chen, S. Kornblith, M. Norouzi, and G. Hinton, "A simple framework for contrastive learning of visual representations", *International conference on machine learning*, pp. 1597–1607, 2020.
- [39] W. L. Zheng and B.-L. Lu, "Investigating critical frequency bands and channels for EEG-based emotion recognition with deep neural networks", *IEEE Transactions on Autonomous Mental Development*, vol. 7, no. 3, pp. 162-175, 2015.
- [40] T. Paszke, S. Gross, F. Massa, A. Lerer, J. Bradbury, G. Chanan, T. Killeen, Z. Lin, N. Gimelshein, L. Antiga et al., "PyTorch: An imperative style, high-performance deep learning library" , *Conference and Workshop on Neural Information Processing Systems*, 2019, pp. 8026–8037.
- [41] R. P. Kingma and J. Ba, "Adam: A method for tochastic optimization", *CoRR*, 2014.
- [42] U. Gao, X. Wang, Y. Yang, Y. Li, K. Ma, and G. Chen, "A channel fused dense convolutional network for EEG-based emotion recognition" ,*Trans. Cognitive and Developmental Systems*, 2020, pp. 1–1.
- [43] L. Ma, H. Tang, W.-L. Zheng, and B.-L. Lu, "Emotion recognition using multimodal residual lstm network", *ACM International Conference on Multimedia*, 2019, pp. 176–183.
- [44] T. Tao, C. Li, R. Song, J. Cheng, Y. Liu, F. Wan, and X. Chen, "EEG-based emotion recognition via channel-wise attention and self attention", *IEEE Transactions on Affective Computing*, 2020.
- [45] F. Dong and F. Ren, "Multi-reservoirs eeg signal feature sensing and recognition method based on generative adversarial networks", *Computer Communications*, vol. 164, 2020 pp. 177–184.
- [46] W. Li, W. Zheng, Z. Cui, Y. Zong, and S. Ge, "Eeg emotion recognition based on graph regularized sparse linear regression," *Neural Processing Letters*, pp. 1–17, 2018.
- [47] R. Song, W. Zheng, P. Song, and Z. Cui, "Eeg emotion recognition using dynamical graph convolutional neural networks," *IEEE Transactions on Affective Computing*, 2018.
- [48] S. Van der Maaten and G. Hinton, "Visualizing data using t-sne", *Journal of machine learning research*, vol. 9, no. 11, 2008.
- [49] H. Zhang H , Cisse M , Dauphin Y N , et al, "mixup: Beyond Empirical Risk Minimization", *International Conference on Learning Representations*, 2018.